doi:10.1093/brain/awn280 *Brain* (2008), **131**, 3266–3276

Mapping local hippocampal changes in Alzheimer's disease and normal ageing with MRI at 3 Tesla

Giovanni B. Frisoni,[1,2] Rossana Ganzola,[1] Elisa Canu,[1] Udo Rüb,[3] Francesca B. Pizzini,[4] Franco Alessandrini,[4] Giada Zoccatelli,[4] Alberto Beltramello,[4] Carlo Caltagirone[5] and Paul M. Thompson[6]

[1]LENITEM - Laboratory of Epidemiology Neuroimaging & Telemedicine, [2]Psychogeriatric Ward, IRCCS Centro San Giovanni di Dio FBF, The National Centre for Research and Care of Alzheimer's and Mental Diseases, Brescia, Italy, [3]Institute for Clinical Neuroanatomy, Department of Neurology, Johann Wolfgang Goethe University, Frankfurt/Main, Germany, [4]Service of Neuroradiology, Ospedale Maggiore, Borgo Trento, Verona, Italy, [5]IRCCS Fondazione Santa Lucia, Rome and [6]Laboratory of Neuroimaging, Department of Neurology, UCLA School of Medicine, Los Angeles, CA 90095, USA

Correspondence to: Giovanni B. Frisoni, MD, Laboratory of Epidemiology Neuroimaging & Telemedicine, IRCCS Centro San Giovanni di Dio FBF - The National Centre for Research and Care of Alzheimer's and Mental Diseases, via Pilastroni 4, 25125 – Brescia, Italy
E-mail: gfrisoni@fatebenefratelli.it

Histological studies have suggested differing involvement of the hippocampal subfields in ageing and in Alzheimer's disease. The aim of this study was to assess *in vivo* local hippocampal changes in ageing and Alzheimer's disease based on high resolution MRI at 3 Tesla. T_1-weighted images were acquired from 19 Alzheimer's disease patients [age 76 ± 6 years, three males, Mini-Mental State Examination 13 ± 4] and 19 controls (age 74 ± 5 years, 11 males, Mini-Mental State Examination 29 ± 1). The hippocampal formation was isolated by manual tracing. Radial atrophy mapping was used to assess group differences and correlations by averaging hippocampal shapes across subjects using 3D parametric surface mesh models. Percentage difference, Pearson's *r*, and significance maps were produced. Hippocampal volumes were inversely correlated with age in older healthy controls ($r = 0.56$ and 0.6 to the right and left, respectively, $P < 0.05$, corresponding to 14% lower volume for every 10 years of older age from ages 65 to 85 years). Ageing-associated atrophy mapped to medial and lateral areas of the tail and body corresponding to the CA1 subfield and ventral areas of the head corresponding to the presubiculum. Significantly increased volume with older age mapped to a few small spots mainly located to the CA1 sector of the right hippocampus. Volumes were 35% and 30% smaller in Alzheimer's disease patients to the right and left ($P < 0.0005$). Alzheimer's disease-associated atrophy mapped not only to CA1 areas of the body and tail corresponding to those also associated with age, but also to dorsal CA1 areas of the head unaffected by age. Regions corresponding to the CA2–3 fields were relatively spared in both ageing and Alzheimer's disease. Hippocampal atrophy in Alzheimer's disease maps to areas in the body and tail that partly overlap those affected by normal ageing. Specific areas in the anterior and dorsal CA1 subfield involved in Alzheimer's disease were not in normal ageing. These patterns might relate to differential neural systems involved in Alzheimer's disease and ageing.

Keywords: Alzheimer's disease; ageing; magnetic resonance; hippocampus; 3D-shape

Received March 18, 2008. Revised September 16, 2008. Accepted October 6, 2008. Advance Access publication November 6, 2008

Introduction

The hippocampus has a key role in Alzheimer's disease. Although the definition of 'hippocampal dementia' (Ball *et al.*, 1985) has been greatly expanded and revised in the last 20 years, this structure remains nevertheless central to the understanding of the disease pathophysiology due to its role in the consolidation of memory, and sensitivity to the pathological lesions of Alzheimer's disease.

Under the assumption that the deposition of pathology leads to neuronal death and hippocampal tissue loss, much work has been conducted to appreciate atrophic changes of the hippocampus *in vivo*. Early computed tomography studies focused on indirect and direct signs such as the dilation of the temporal horns and thinning of the medial temporal lobe, and subjective rating scales were developed based on MRI as well as linear measures and protocols for

© The Author (2008). Published by Oxford University Press on behalf of the Guarantors of Brain. All rights reserved. For Permissions, please email: journals.permissions@oxfordjournals.org

Downloaded from https://academic.oup.com/brain/article/131/12/3266/296136 by guest on 20 April 2024

volumetric measurements (Frisoni *et al*., 1996; Frisoni *et al*., 2002; Bosscher and Scheltens, 2002). Such markers of medial temporal atrophy have been proposed mainly as diagnostic tools to improve the accuracy of the diagnosis of Alzheimer's disease and to predict the development of Alzheimer's disease in persons with mild cognitive impairment (Jack *et al*., 1992), but have proved of little value to further the understanding of the pathophysiology.

Due to their intrinsic technical limitations, the above markers regard the hippocampus as a unitary structure, although this is hardly the case. The hippocampus, including strictly speaking subfields CA1–CA4, and the hippocampal formation, including also dentate gyrus, fimbria, subiculum and parasubiculum, is a highly sophisticated structure. Stimuli coming from the entorhinal cortex are processed by the dentate gyrus, subfields CA4 and CA3, before being projected outside the medial temporal lobe via CA1 or subicular efferent projections. Moreover, in addition to the unsurprising right–left specialization for verbal and visuospatial material (Papanicolaou *et al*., 2002), some degree of anterior-to-posterior specialization has been shown by fMRI studies (Strange *et al*., 1999).

The first attempt to detect local atrophic changes within the hippocampus in Alzheimer's disease that we are aware of dates back to the year 2000, when on 1.5T images Laakso and colleagues divided the volume of the hippocampus into anterior, middle and posterior sectors and found that volume reduction in Alzheimer's disease was equally distributed, while atrophy in frontotemporal dementia patients spared the middle and posterior sectors (Laakso *et al*., 2000). More sophisticated probing tools based on diffeomorphic and mesh modelling but again on 1.5T images, were later able to map atrophic changes to areas of the surface of the hippocampal formation corresponding to the CA1 sector and part of the subicular area (Csernansky *et al*., 2000; Thompson *et al*., 2004; Frisoni *et al*., 2006). Scanty *in vivo* data on 1.5T images are available on the local hippocampal changes associated with healthy ageing (Wang *et al*., 2003). The contrast-to-noise ratio of 3T, twice that of 1.5T scanners, might significantly enhance the accuracy of mapping local hippocampal volume changes in patients with Alzheimer's disease and normal older persons. Although, shape analysis of the hippocampus at 3T has been carried out in autism, alcohol abuse and hippocampal sclerosis (Beresford *et al*., 2006; Nicolson *et al*., 2006; Eriksson *et al*., 2008), this has never been carried out in Alzheimer's disease and healthy ageing.

The major goal of this study is to map the local structural changes that take place in the hippocampus of patients with Alzheimer's disease and assess their specificity towards healthy aging with the hypothesis that different hippocampal subregions are affected in Alzheimer's disease and ageing. To this avail, state-of-the-art 3T hardware for image collection has been used paired with an image post-processing algorithm based on 3D parametric surface mesh models. This approach, although requiring manual segmentation, has the advantage over less human-dependent techniques such as tensor-based morphometry (TBM) and voxel-based morphometry of much greater spatial accuracy (Leow *et al*., 2005; Hua *et al*. 2008; Morra *et al*., 2008).

Methods

Subjects

The study population consisted of 14 patients with moderate to severe probable Alzheimer's disease, diagnosed according to NINCDS-ADRDA criteria (McKhann *et al*., 1984), and 14 healthy volunteers. Alzheimer's disease patients were recruited within a pharmaco fMRI study of memantine; data reported here are those at baseline. Patients were taken from those seen at the IRCCS Centro S. Giovanni di Dio Fatebenefratelli, in Brescia, Italy. Patients with clinical dementia rating of 2 or greater were included and patients scoring higher than 4 on Hachinski modified scale were excluded (Rosen *et al*., 1980). Global cognitive function was assessed with the Mini-Mental State Examination (MMSE) (Folstein *et al*., 1975). Normal controls were mostly patients' non-consaguineous relatives of similar age and no history of transitory ischemic attack (TIA) or stroke, head trauma, alcohol and substance abuse, corticosteroid therapy or recent weight loss. Standardized history taking, behavioural and functional assessment, physical and neurological examination and a comprehensive neuropsychological battery adequate to patients' cognitive impairment severity were carried out for all participants. The full neuropsychological battery included the coloured Raven's matrices, logical memory test, Rey's figure copy and recall, digit span, Corsi's spatial span, token test, letter and category fluency and trail making test. The original case report form of the clinical assessment may be accessed at http://www.centroalzheimer.it/Public/ProtocolloMEM_T0.doc (in Italian).

Table 1 shows that the two groups were not significantly different for age. Patients had 3 years less education, and included fewer males than controls. Controls spanned an age window of 15 years (66 to 81 years). The MMSE of patients spanned a large window of cognitive performance, from severe (MMSE 5/30) to mild impairment (MMSE 21/30), but were on average of moderate severity. Hippocampal volumes of Alzheimer's disease patients were consistent with expectations, exhibiting 30% and 35% tissue loss to the left and right relative to controls.

Written informed consent was obtained from all patients and normal controls or their primary caregivers, after discussion of the participation risks and benefits. No compensation was provided. The study was approved by the local ethics committee.

Magnetic resonance acquisition

The 3D high-resolution T_1-weighted MRIs were acquired on a 3.0 T Siemens Allegra scanner at the Neuroradiology Unit of the Ospedale Maggiore Borgo Trento, Verona, Italy, with a standard head coil. Scans were acquired with gradient echo 3D technique with the following acquisition protocol: repetition time (TR) = 2300 ms, echo time (TE) = 3.93 ms, inversion time (TI) = 1100 ms, flip angle = 12°, gap = 50%, voxel = 1 × 1 × 1 mm, acquisition matrix = 256 × 256, slice thickness = 1 mm, total number of slices = 160, acquisition time 8′ 37″.

Image processing

Images were reoriented along the anterior commissure (AC)–posterior commissure (PC) line, all voxels below the cerebellum

Downloaded from https://academic.oup.com/brain/article/131/12/3266/296136 by guest on 20 April 2024

Table 1 Socio-demographic and clinical features of moderate to severe Alzheimer's disease patients and older healthy controls

	Alzheimer's disease ($n = 19$)	Controls ($n = 19$)	P
Age, years	76.1 ± 5.7 [66–86]	73.6 ± 5.5 [66–82]	NS
Sex, male	3 (16%)	11 (58%)	0.017
Education, years	5.3 ± 2.1 [3–13]	8.7 ± 4.0 [3–17]	0.002
MMSE	13.1 ± 3.8 [5–21]	28.6 ± 1.1 [27–30]	<0.0005
Hippocampal volume (mm^3)			
Right	2745 ± 737 [1689–4171]	4216 ± 651 [3027 ± 5534]	<0.0005
Left	2705 ± 785 [1230–3950]	3889 ± 634 [2806–5270]	<0.0005

Figures denote means ± SD [range] or n (%). P denotes significance on t-or χ^2-test.
Hippocampal volumes were normalized to cranial size of a reference template (see 'Methods section').
NS = not significant.

were removed with MRIcro (www.psychology.nottingham.ac.uk/staff/cr1/mricro.html) and the spatial coordinate origin was manually set to the anterior commissure. Images were normalized with the Statistical Parametric Mapping (SPM2) software (www.fil.ion.ucl.ac.uk/spm) to a customized template made of all patients and all controls with a linear (12 parameters) transformation to preserve local shape differences in anatomy across subjects so that they could be quantified in standardized space. Warping of one hippocampus to another was based on matching homologous points on a rectilinear surface mesh adapted to the structure boundary.

The hippocampi were manually traced on the reoriented and normalized images. A single tracer blind to diagnosis (R.G.) outlined the hippocampal boundaries on contiguous coronal 1.0 mm thick sections following a standardized and validated protocol (Pruessner *et al.*, 2000) using an interactive software program developed at the LONI (Laboratory of NeuroImaging), University of California at Los Angeles (http://www.loni.ucla.edu/ICBM/ICBM_ResSoftware.html#seg3). Tracings included the hippocampus proper, dentate gyrus, subiculum (subiculum proper and presubiculum), alveus and fimbria (Fig. 1). Each hippocampus comprised approximately 30–40 consecutive slices, and tracing took about 40 min per subject. Normalized hippocampal volumes were obtained from the tracings on normalized images and retained for statistical analyses. Test–retest reliability on 20 subjects was good—intra-class correlation coefficients were 0.92 for the left and 0.86 for the right hippocampus.

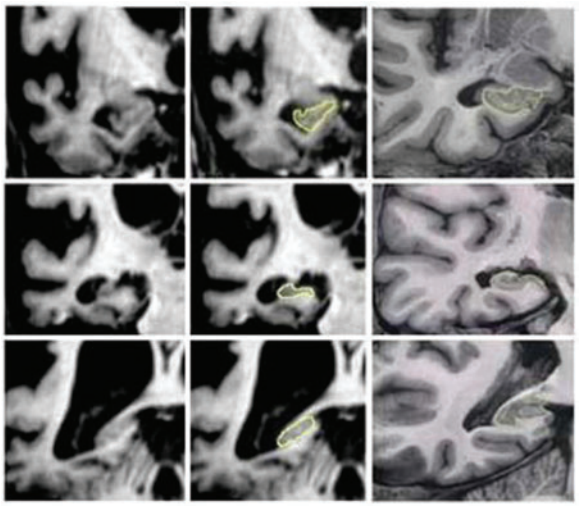

Fig. 1 Manual tracing of the hippocampal formation in an Alzheimer's patient. Selected slices are shown at the level of the head (upper row), body (mid row) and tail (lower row). The left column shows native and the mid column traced scans. The right column shows a gross pathological specimen of a normal person taken from Duvernoy (1998) where the boundaries of the hippocampus have been traced.

Radial atrophy mapping

The 3D parametric surface mesh models were created from the manual tracings of hippocampal boundaries (Narr *et al.*, 2004; Thompson *et al.*, 2004). This procedure allows measurements to be made at corresponding surface locations in each subject, which are then compared statistically in 3D (Thompson *et al.*, 1996). The 3D parametric mesh models of each individual's hippocampi were analysed to estimate local hippocampal volume loss in Alzheimer's disease compared with controls. To assess hippocampal morphology, a medial curve was automatically defined as the 3D curve traced out by the centroid of the hippocampal boundary in each image slice. The radial size of each hippocampus at each boundary point was assessed by automatically measuring the radial 3D distance from the surface points to the medial curve defined for individual's hippocampal surface model. Distance fields indexing local expansions or contractions in hippocampal surface morphology were statistically compared between groups at equivalent hippocampal surface points in 3D space (Thompson *et al.*, 2004).

It needs to be underlined that this technique may not work optimally in conditions where volumetric changes are symmetric and opposite, i.e. if atrophy occurred in the dorsal side while volume increase occurred in the ventral side, this could result in a non-significant finding due to the shifting of the centroid. However, growth is not expected in aging or Alzheimer's disease. Moreover, the use of the central axis is a strength as unlike automated registration methods such as voxel-based morphometry, it will be invariant to shifting of the structure in space, thus resulting in more accurate registration.

Statistical analysis

Atrophy maps were generated on 3D models of the hippocampal formation where the dorsal and ventral surfaces can be appreciated indicating local group differences in radial distance. The percent change relative to controls and the associated P-value maps were plotted onto a colour-coded model of the hippocampal surface. The statistical test for the group difference Alzheimer's disease

Downloaded from https://academic.oup.com/brain/article/131/12/3266/296136 by guest on 20 April 2024

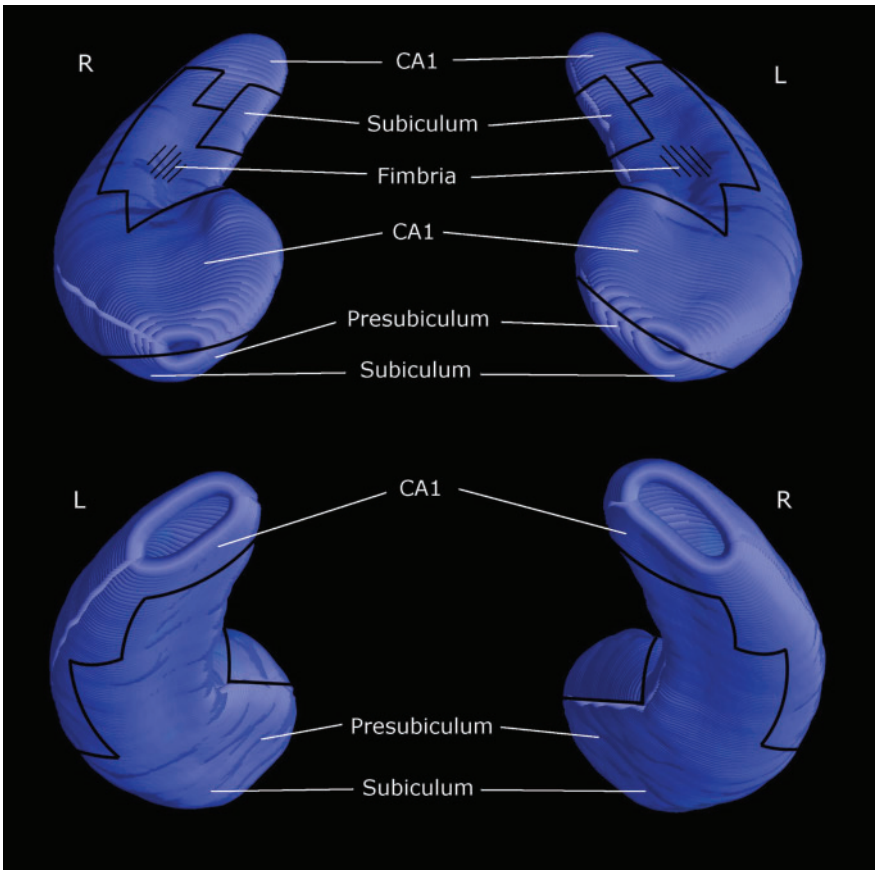

Fig. 2 Cytoarchitectonic subregions mapped on blank MR-based models at 3T of the hippocampal formation of a healthy subject (Frisoni *et al.*, 2006).

versus controls was formulated as a two-tailed *t*-test (unpaired) at each surface vertex on the hippocampus, in which the radial distance values for each group were compared and the associated *P*-value computed and plotted as a measure of the effect size at each location, while separating positive and negative effects. For the correlation maps, the statistics were computed using linear regression at each surface vertex on the hippocampus.

Cytoarchitectural subfields were mapped onto the models based on an atlas where these are shown together with the corresponding magnetic resonance (MR) sections (Duvernoy, 1998; Frisoni *et al.*, 2006) (Fig. 2). Age was used as covariate to generate 3D maps of correlations with atrophy in healthy controls alone.

Overall *P*-values were computed for the left and right hippocampal formation maps using a permutation testing approach, measuring the distribution of features in statistical maps that would be observed by accident if the subjects were randomly assigned to groups (Thompson *et al.*, 2003). The overall *P*-value in permutation testing was computed by comparing the number of voxels exceeding a statistical threshold (the suprathreshold cluster was defined as voxels with significance $P<0.01$) in the true labelling to the permutation distribution. This provides an approximate corrected *P*-value for the effects in the overall map, and intuitively it may be interpreted as the proportion of randomized maps that 'beat' the true map. The number of permutations N was chosen to control the standard error SE_P of omnibus probability P, which follows a binomial distribution (Edgington, 1995). We selected $N>8000$ tests out of the total number of possible permutations ($\approx 10^{23}$) such that the approximate margin of error (95% confidence interval) for P was around 5% of P, and 0.05 was chosen as the significance level.

Results

Effect of ageing and Alzheimer's disease on total hippocampal volumes

Figure 3 details the distribution of normalized hippocampal volumes in patients and controls across age, showing that at any age, the volumes for patients tended to be lower than controls', despite some overlap. This was true mainly to the right where 13/19 Alzheimer's disease patients (68%) were below the 95% confidence limit for controls (sensitivity and specificity of 68% and 95%), while overlap was more substantial to the left (sensitivity and specificity of 53% and 95%). Mean hippocampal volumes in older controls decreased by 14% per decade between the ages of 65 and 85 years.

Effect of ageing on local hippocampal volumes

Figure 4A shows that in controls older age was correlated with significant changes of hippocampal shape ($P=0.05$ and $P=0.01$ by permutation test for the left and right).

Downloaded from https://academic.oup.com/brain/article/131/12/3266/296136 by guest on 20 April 2024

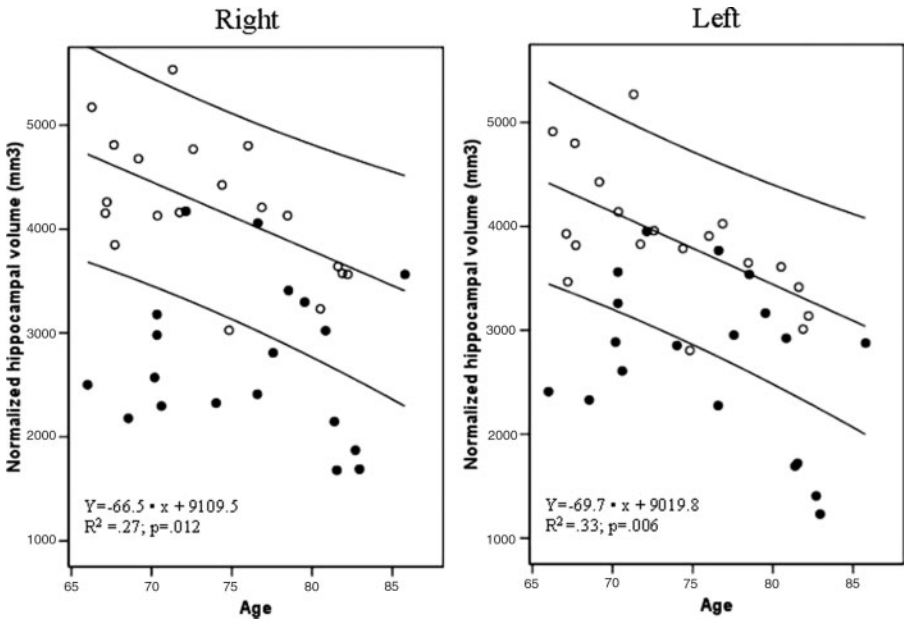

Fig. 3 Effect of ageing and Alzheimer's disease on total hippocampal volume in 19 Alzheimer's patients (closed circle) and 19 older healthy controls (open circle). Regression lines of volume on age in controls and 95% confidence bounds of the distribution are shown as well as regression equations, percent explained variance (R^2) and significance (P).

Greater volume with older age mapped to small spots mainly to the right, located in the CA1, CA2–3 and subicular sectors of which only few voxels were significant. Lower volume with older age mapped mainly to medial and lateral regions in the body and tail encompassing the CA1 subfield. Subicular regions were affected bilaterally. Atrophy mapping to the dorsal aspect in the CA2–3 subfield proved to be significant in only a few voxels.

In order to directly compare the effect of older age with that of Alzheimer's disease (see 'Topographic overlap between ageing and Alzheimer's' section), percent difference maps and significance maps (Fig. 4B) were computed ($P = 0.04$ and $P = 0.03$ by permutation test for the left and right) by contrasting the 9 older (age 78.6 ± 3.1, hippocampal volume $3482 \pm 420\,mm^3$ to the left and 3844 ± 581 to the right) to the 10 younger control subjects (age 69.1 ± 2.2, hippocampal volume 4254 ± 576 and 4551 ± 532). As expected, these were remarkably similar to the correlation maps (Fig. 4A).

Effect of Alzheimer's on local hippocampal volumes

The dorsal surface of the hippocampus showed atrophy in a large area encompassing most of the CA1 subfield, only the medial part of the hippocampal head being spared by atrophy (Fig. 5) and showed, on the contrary, a small and non-significant bulging. The area corresponding to the CA2–3 subfields was remarkably, although not altogether spared and again showed non-significant bulging in its posterior most part. On the ventral surface, the presubiculum was more affected than the subiculum in the head bilaterally, and in the body and tail a longitudinal strip in the subiculum was spared encompassing the midline. The permutation test was highly significant ($P < 0.0005$) on both sides.

Topographic overlap between ageing and Alzheimer's

Table 2 shows a synopsis of the areas affected by atrophy in normal ageing and Alzheimer's disease. Figure 6 shows that the areas of substantial overlap between ageing- and Alzheimer's-associated atrophy were located mainly in the medial and lateral aspects of the tail bilaterally (Fig. 6C, left columns). In the dorsal aspect of the head and right presubiculum, ageing- and Alzheimer's-associated atrophy were never overlapping (Fig. 6C), while areas of overlap were present in the subicular/presubicular region in the head and body mainly to the left (Fig. 6C, right columns).

Discussion

Using high-resolution images acquired on a 3T scanner, we found that the hippocampus of Alzheimer's disease patients shows a topographic pattern of shape changes distinct only in part from that of healthy ageing. The dorsolateral aspect of the head (CA1 subfield) and the presubicular part of the head were affected only in Alzheimer's disease, the lateral part of the subiculum in the head was affected only in ageing and the lateral and medial aspects of the tail (CA1) were affected in both Alzheimer's disease and ageing. To our knowledge, this is the first study directly comparing the local changes that take place in the hippocampus during

Downloaded from https://academic.oup.com/brain/article/131/12/3266/296136 by guest on 20 April 2024

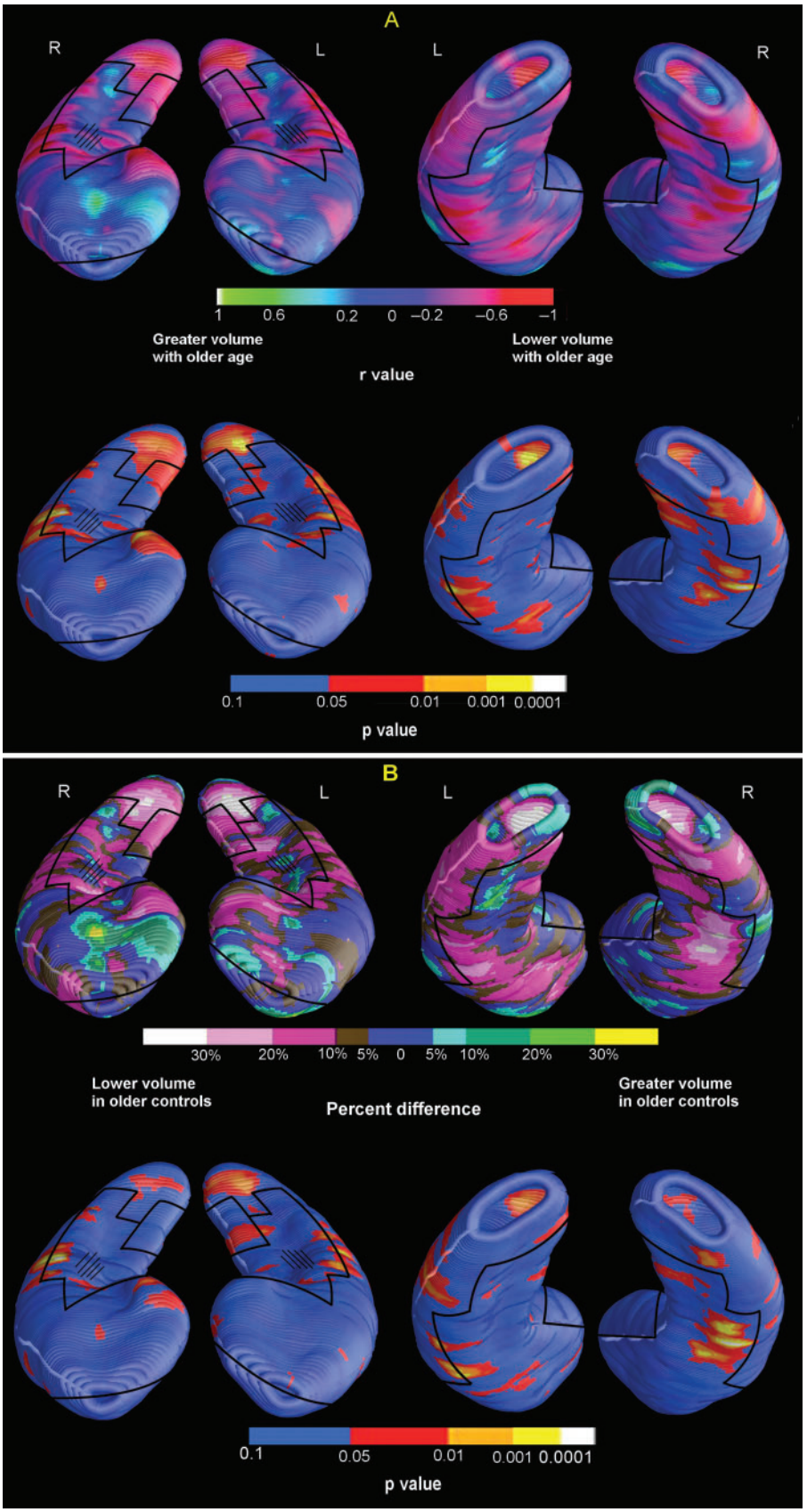

Fig. 4 Effect of ageing on local hippocampal volume. (**A**) Correlation (Pearson's *r* and significance) between age and local volume in 19 older healthy controls. (**B**) Percent difference and significance of local volume between 9 older and 10 younger healthy controls.

Downloaded from https://academic.oup.com/brain/article/131/12/3266/296136 by guest on 20 April 2024

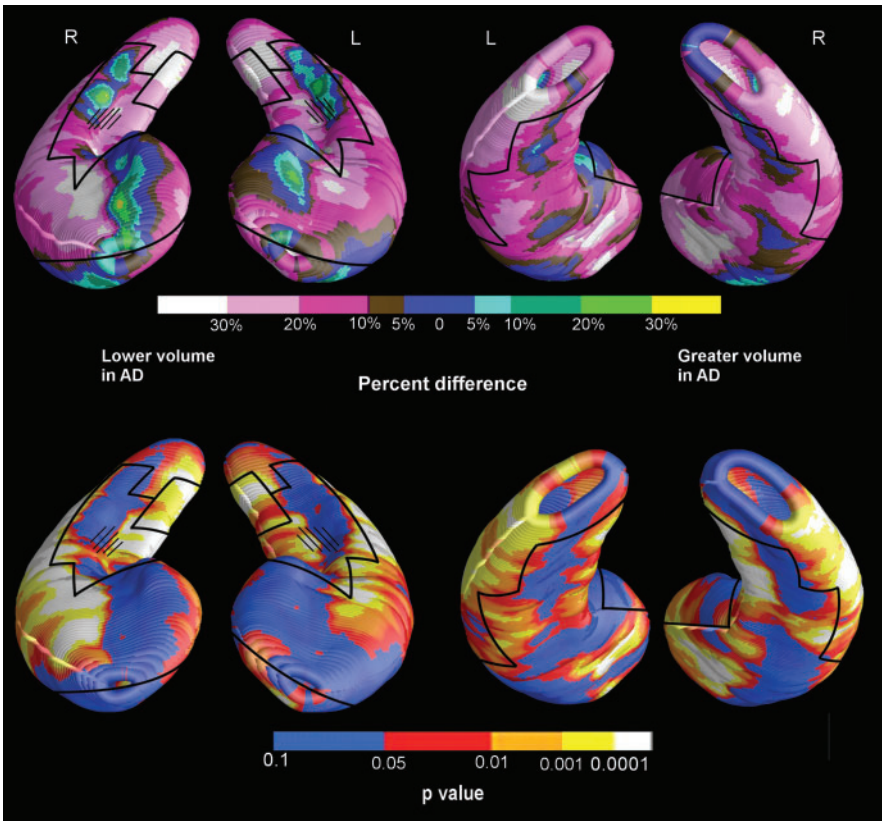

Fig. 5 Effect of Alzheimer's disease on local hippocampal volume: maps of the difference of regional volume between 19 Alzheimer's disease patients and 19 older healthy controls.

Table 2 Synopsis of local hippocampal changes in normal ageing and Alzheimer's disease

	Normal ageing	Alzheimer's disease
Presubiculum		
Head	0/−	− −/− − −
Subiculum		
Head	0/−	−/0
Body	+/− − −	0/− −
Tail	±/∓	0/− − −
CAI		
Head	+/0 (lateral) +/− (medial)	±/− − − (lateral) + + +/0 (medial)
Body	+ + +/−	−/− −
Tail	− −/− − −	− −/− − −
CA2-3		
Body	0/−	− −/+ +
Tail	±/∓	0/+ +

Box shows the correspondence of marks with percentage change

normal ageing and in Alzheimer's disease. The use of high field MR imaging is also novel.

The results of the present study of Alzheimer's disease are in agreement with our own previous work with the same mapping technique on an independent group of mild to moderate patients scanned with a lower field strength (1.0T) scanner (Frisoni *et al.*, 2006), and with results from other groups (Wang *et al.*, 2003; Apostolova *et al.*, 2006; Becker *et al.*, 2006). With a completely different shape analysis algorithm applied to 1.5T images, the Washington University group of Csernansky and colleagues prospectively studied mild Alzheimer's disease patients and healthy older persons and found that atrophy affected the dorsal aspect of the hippocampus in the same CA1 areas that we found to be affected. In particular, the head was atrophic in its lateral but not in its medial part (Wang *et al.*, 2003). A later study by the UCLA group (Apostolova *et al.*, 2006) confirmed these findings and further refined the description of the changes in the subiculum and presubiculum: in agreement with the present findings, their comparison of mild cognitive impairment (MCI) patients converting to Alzheimer's disease with those improving shows that in the body and tail the subicular area is spared in a region encompassing the midline. These findings in the subiculum and presubiculum were confirmed by a population-based study in the Honolulu Asia aging study (HAAS) cohort on 24 Alzheimer's disease

Downloaded from https://academic.oup.com/brain/article/131/12/3266/296136 by guest on 20 April 2024

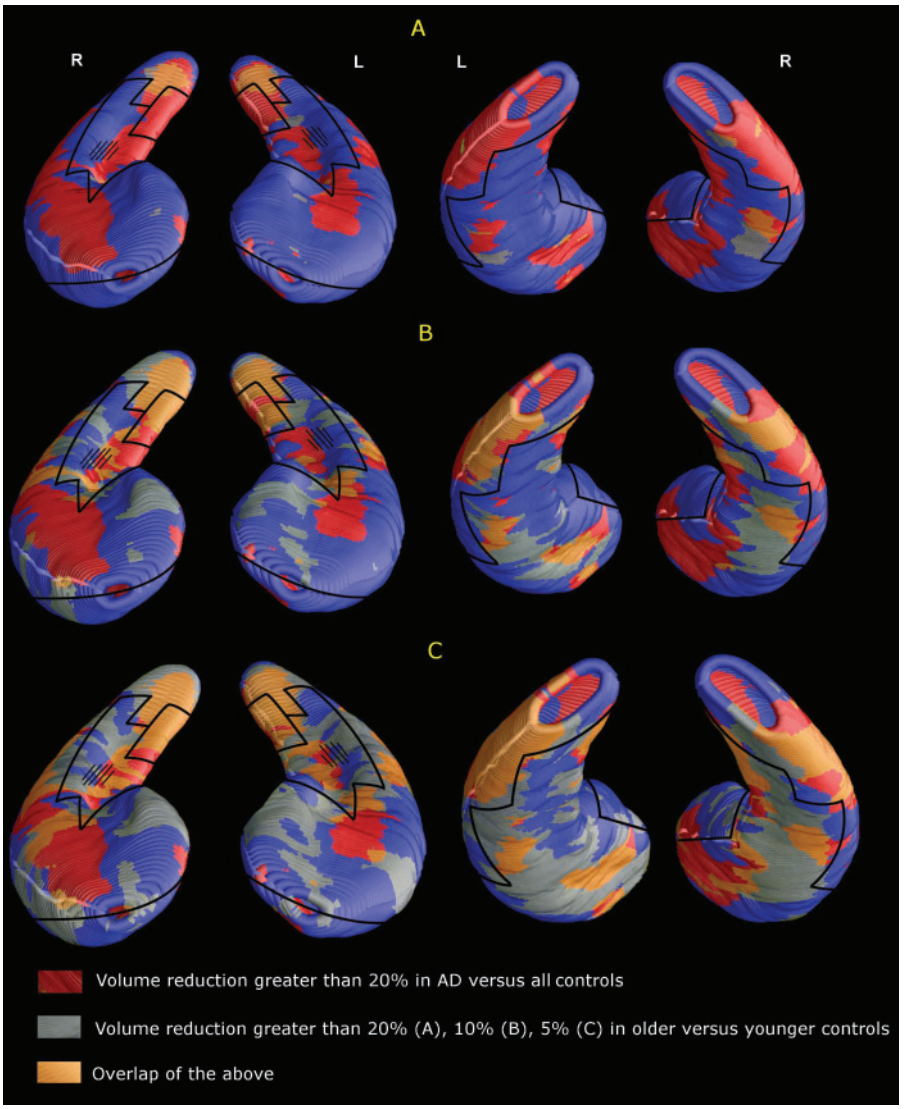

Fig. 6 Topographic overlap between ageing- and Alzheimer's-associated local hippocampal atrophy. Red areas denote tissue loss greater than 20% in Alzheimer's disease patients compared with all controls, gray areas those of 9 older compared with 10 younger controls, and orange areas the overlap of the previous.

patients and 102 controls (Scher *et al.*, 2007) and again by Wang and colleagues in 49 very mild Alzheimer's disease patients and 86 non-demented older persons (Wang *et al.*, 2006).

The hippocampus is affected early in Alzheimer's disease by neurofibrillary tangle deposition, spreading from the entorhinal cortex to the CA1 subfield and subicular region, then to the CA2–3 subfields, the CA4 subfield and finally the neocortex (Schonheit *et al.*, 2004). Therefore, while involvement of the subiculum/presubiculum and CA1 subfield with sparing of CA2–3 subfields can easily be accounted for and has been confirmed *in vivo* with *ad hoc* MR image acquisition protocols (Adachi *et al.*, 2003), the local differences within subfields are less easily explained. In particular, why in the head are the medial dorsal aspect of CA1 and the ventrolateral (subicular) area spared? And why in the body and tail, is a longitudinal strip in the subiculum encompassing the midline also spared? It is tempting to hypothesize that these non-atrophic areas correspond at least in part to the presubiculum, believed to be relatively spared in Alzheimer's disease (Hyman *et al.*, 1984; Van Hoesen and Hyman, 1990). While functional differences of the anterior versus posterior hippocampus are well known (Strange *et al.*, 1999), those in the transverse dimension (medial versus lateral) have been less deeply investigated. Pathological studies show that the CA1 subfield, subiculum proper and entorhinal cortex have a somatotopic organization. CA1 cells located closest to CA2 tend to innervate the most distal portion of the subiculum (closest to the presubiculum), whereas CA1 cells located close to the subiculum projected just across the CA1 subicular border (Tamamaki and Nojyo, 1990; Amaral *et al.*, 1991). In the rat, projections originating from subicular cells close to CA1, i.e. lateral ventral hippocampal region, terminate

Downloaded from https://academic.oup.com/brain/article/131/12/3266/296136 by guest on 20 April 2024

exclusively in the lateral entorhinal cortex and in the perirhinal cortex, while projections from cells closer to the subiculum–presubiculum border, i.e. medial distal part of subiculum terminate in the medial entorhinal cortex (Kloosterman *et al.*, 2003). These observations indicate that the subicular and presubicular cortex have a different structure and, likely, function, but how this should be interpreted in the framework of Alzheimer's disease symptoms will need to be elucidated in future studies.

The interpretation of our results in aged cognitively healthy people in light of previous *in vivo* and pathologic studies is even more arduous, given the scant literature available. Cellular and neurochemical changes in the hippocampus with ageing show remarkable heterogeneity in that decremental changes are not invariable in all hippocampal structures. For example, pyramidal cells are lost in the subiculum between age 30 and 60 years (Trillo and Gonzalo, 1992), but stabilize thereafter (West and Gundersen, 1990; Trillo and Gonzalo, 1992), while cell loss in the presubiculum and CA1 subfield is more linearly associated with increasing age at least until the mid-eighties (West and Gundersen, 1990; Trillo and Gonzalo, 1992). Although, this observation is inconsistent with our finding of greater atrophy in the subicular than presubicular region in our cognitively healthy persons aged 58 to 81 years, the *in vivo* study by Wang and colleagues (Wang *et al.*, 2003) using MRI reported findings consistent with our own. That study found that normal ageing is associated with atrophy of the lateral and medial aspects of the tail in an area largely encompassing the CA1 subfield, and that atrophy in the dorsal aspect of the head maps to regions distinct from those atrophic in Alzheimer's disease (Wang *et al.*, 2003).

Strengths of the present study are the use of images acquired at 3T and the image post-processing technique with surface mesh modelling. Studies of the hippocampus at 3T are still but few. Briellmann and colleagues (Briellmann *et al.*, 2001) have compared the accuracy of 1.5 and 3T scanning to study the hippocampus in eight adult healthy persons scanned twice at both 1.5 and 3T. They manually segmented the hippocampi, and showed that hippocampal volumes were not different. However, this finding is not surprising since the computation of overall hippocampal volume averages out the error variance of local tracing, whatever its size. On the contrary, in the case of shape analysis decreasing the error variance of local tracing is of the greatest relevance to enhance the accuracy of topographic localization of the local volumetric changes. It is therefore reasonable that the greater tissue contrast in 3T scans may be beneficial to shape analysis. Shape analysis at 3T has been carried out in autism, alcohol abuse and hippocampal sclerosis (Beresford *et al.*, 2006; Nicolson *et al.*, 2006; Eriksson *et al.*, 2008) showing relatively specific patterns of shape changes, but the present is the first study that we are aware of on ageing and Alzheimer's disease.

The surface mesh modelling that we used in the present study, although requiring segmentation of the hippocampus by a human hand, has some advantages over automated voxel-based methods. For purposes of comparison, we previously computed hippocampal volume from TBM, which estimates anatomical structure volumes from a deformation transform that re-shapes a mean anatomical template onto each individual scan (Morra *et al.*, 2008) in a group of seven controls, seven MCI and seven Alzheimer's disease patients and found that TBM-derived hippocampal volume measures correlated poorly with MMSE score ($r = 0.126$; $P > 0.05$). Some reasons why TBM may not be optimal for hippocampal volumetric study are detailed elsewhere (Becker *et al.*, 2006; Frisoni *et al.*, 2006; Hua *et al.*, 2008). TBM is typically best for assessing differences at a scale greater than 3–4 mm (the typical resolution of the spectral representation used to compute the deformation field) (Leow *et al.*, 2005; Hua *et al.*, 2008). For smaller scale effects, direct modelling of the structure, e.g. using surface-based geometrical methods, may offer additional statistical power to detect subregional differences. Direct assessments of hippocampal volume by our radial mapping algorithm correlated better than TBM with MMSE scores, and explained a substantial proportion of their variance even in this relatively small sample ($r \sim 0.6$; $P < 0.01$).

Some limitations of this study should be acknowledged. First, the small number of subjects is certainly something that future studies on larger datasets such as that of the Alzheimer's Disease Neuroimaging Initiative will be able to address. Second, our sample of cognitively healthy older persons allowed us to assess age effects only in the restricted age window between 67 and 75 years. Third, cases and controls were not well balanced for gender. The effect of gender on hippocampal morphology is, if any, much lower than that of ageing and Alzheimer's disease. Some studies suggest greater hippocampal volumes in men (Murphy *et al.*, 1996), others in women (Golomb *et al.*, 1993, Pruessner *et al.*, 2001) and others no effect (Coffey *et al.*, 1998; Jack *et al.*, 1998), so better matching will allow more accurate estimates. Lastly, the small group size for the Alzheimer's disease patients prevented the study of the effect of disease severity on local atrophy and, as a consequence, the chronology of atrophy progression in Alzheimer's disease and normal ageing.

Funding

Italian Ministry of Health, Ricerca Finalizzata 'Malattie neurodegenerative legate all'invecchiamento: dalla patogenesi alle prospettive terapeutiche per un progetto traslazionale' (grant no. 125/2004); Lundbeck Italia SPA Pharmaceuticals.

References

Adachi M, Kawakatsu S, Hosoya T, Otani K, Honma T, Shibata A, et al. Morphology of the inner structure of the hippocampal formation in Alzheimer disease. AJNR Am J Neuroradiol 2003; 24: 1575–81.

Downloaded from https://academic.oup.com/brain/article/131/12/3266/296136 by guest on 20 April 2024

Amaral DG, Dolorfo C, Alvarez-Royo P. Organization of CA1 projections to the subiculum: a PHA-L analysis in the rat. Hippocampus 1991; 1: 415–35.

Apostolova LG, Dutton RA, Dinov ID, Hayashi KM, Toga AW, Cummings JL, et al. Conversion of mild cognitive impairment to Alzheimer disease predicted by hippocampal atrophy maps. Arch Neurol 2006; 63: 693–9.

Ball MJ, Fisman M, Hachinski V, Blume W, Fox A, Kral VA, et al. A new definition of Alzheimer's disease: a hippocampal dementia. Lancet 1985; 1: 14–6.

Becker JT, Davis SW, Hayashi KM, Meltzer CC, Toga AW, Lopez OL, et al. Three-dimensional patterns of hippocampal atrophy in mild cognitive impairment. Arch Neurol 2006; 63: 97–101.

Beresford TP, Arciniegas DB, Alfers J, Clapp L, Martin B, Du Y, et al. Hippocampus volume loss due to chronic heavy drinking. Alcohol Clin Exp Res 2006; 30: 1866–70.

Bosscher L, Scheltens P. MRI of the medial temporal lobe for the diagnosis of Alzheimer' Disease. In: Quizilbash N, Schneider LS, Chui H, Tariot P, Brodaty H, Kaye J, et al. editors. Evidence-based dementia practice. Oxford: Blackwell Publishing; 2002. p. 154–62.

Briellmann RS, Syngeniotis A, Jackson GD. Comparison of hippocampal volumetry at 1.5 tesla and at 3 tesla. Epilepsia 2001; 42: 1021–4.

Coffey CE, Lucke JF, Saxton JA, Ratcliff G, Unitas LJ, Billig B, et al. Sex differences in brain aging: a quantitative magnetic resonance imaging study [review]. Arch Neurol 1998; 55: 169–79.

Csernansky JG, Wang L, Joshi S, Miller JP, Gado M, Kido D, et al. Early DAT is distinguished from aging by high-dimensional mapping of the hippocampus. Neurology 2000; 55: 1636–43.

Duvernoy HM. editor. The human hippocampus. Functional anatomy, vascularization and serial section with MRI. 3rd edn. Berlin: Springer; 1998.

Edgington ES. Randomization tests. New York, NY: Marcel Dekker; 1995.

Eriksson SH, Thom M, Bartlett PA, Symms MR, McEvoy AW, Sisodiya SM, et al. PROPELLER MRI visualizes detailed pathology of hippocampal sclerosis. Epilepsia 2008; 49: 33–9.

Folstein MF, Folstein SE, McHugh PR. 'Mini-mental state'. A practical method for grading the cognitive state of patients for the clinician. J Psychiatr Res 1975; 12: 189–98.

Frisoni GB, Beltramello A, Weiss C, Geroldi C, Bianchetti A, Trabucchi M. Linear measures of atrophy in mild Alzheimer disease. AJNR Am J Neuroradiol 1996; 17: 913–23.

Frisoni GB, Geroldi C, Beltramello A, Bianchetti A, Binetti G, Bordiga G, et al. Radial width of the temporal horn: a sensitive measure in Alzheimer disease. AJNR Am J Neuroradiol 2002; 23: 35–47.

Frisoni GB, Sabattoli F, Lee AD, Dutton RA, Toga AW, Thompson PM. In vivo neuropathology of the hippocampal formation in AD: a radial mapping MR-based study. Neuroimage 2006; 32: 104–10.

Golomb J, de Leon MJ, Kluger A, George AE, Tarshish C, Ferris SH. Hippocampal atrophy in normal aging. An association with recent memory impairment. Arch Neurol 1993; 50: 967–73.

Hua X, Leow AD, Lee S, Klunder AD, Toga AW, Lepore N, et al. 3D characterization of brain atrophy in Alzheimer's disease and mild cognitive impairment using tensor-based morphometry. Neuroimage 2008; 41: 19–34.

Hyman BT, Van Hoesen GW, Damasio AR, Barnes CL. Alzheimer's disease: cell-specific pathology isolates the hippocampal formation. Science 1984; 225: 1168–70.

Jack CR Jr, Petersen RC, O'Brien PC, Tangalos EG. MR-based hippocampal volumetry in the diagnosis of Alzheimer's disease. Neurology. 1992; 42: 183–8.

Jack CR Jr, Petersen RC, Xu Y, O'Brien PC, Smith GE, Ivnik RJ, et al. Rate of medial temporal lobe atrophy in typical aging and Alzheimer's disease. Neurology. 1998; 51: 993–9.

Kloosterman F, Witter MP, Van Haeften T. Topographical and laminar organization of subicular projections to the parahippocampal region of the rat. J Comp Neurol 2003; 455: 156–71.

Laakso MP, Frisoni GB, Könönen M, Mikkonen M, Beltramello A, Geroldi C, et al. Hippocampus and entorhinal cortex in frontotemporal dementia and Alzheimer's disease: a morphometric MRI study. Biol Psychiatry 2000; 47: 1056–63.

Leow A, Huang SC, Geng A, Becker J, Davis S, Toga A, et al. Inverse consistent mapping in 3D deformable image registration: its construction and statistical properties. Inf Process Med Imaging 2005; 19: 493–503.

McKhann G, Drachman D, Folstein M, Katzman R, Price D, Stadlan EM. Clinical diagnosis of Alzheimer's disease: report of the NINCDS-ADRDA Work Group under the auspices of Department of Health and Human Services Task Force on Alzheimer's Disease. Neurology 1984; 34: 939–44.

Morra J, Tu Z, Apostolova LG, Green AE, Avedissian C, Madsen SK, et al. Validation of a fully automated 3D hippocampal segmentation method using subjects with Alzheimer's disease, mild cognitive impairment, and elderly controls. NeuroImage 2008; 43: 59–68.

Murphy DG, DeCarli C, McIntosh AR, Daly E, Mentis MJ, Pietrini P, et al. Sex differences in human brain morphometry and metabolism: an in vivo quantitative magnetic resonance imaging and positron emission tomography study on the effect of aging. Arch Gen Psychiatry 1996; 53: 585–94.

Narr KL, Thompson PM, Szeszko P, Robinson D, Jang S, Woods RP, et al. Regional specificity of hippocampal volume reductions in first-episode schizophrenia. Neuroimage 2004; 21: 1563–75.

Nicolson R, DeVito TJ, Vidal CN, Sui Y, Hayashi KM, Drost DJ, et al. Detection and mapping of hippocampal abnormalities in autism. Psychiatry Res 2006; 148: 11–21.

Papanicolaou AC, Simos PG, Castillo EM, Breier JI, Katz JS, et al. The hippocampus and memory of verbal and pictorial material. Learn Mem 2002; 9: 99–104.

Pruessner JC, Collins DL, Pruessner M, Evans AC. Age and gender predict volume decline in the anterior and posterior hippocampus in early adulthood. J Neurosci 2001; 21: 194–200.

Pruessner JC, Li LM, Serles W, Pruessner M, Collins DL, Kabani N, et al. Volumetry of hippocampus and amygdala with high-resolution MRI and three-dimensional analysis software: minimizing the discrepancies between laboratories. Cereb Cortex 2000; 10: 433–42.

Rosen WG, Terry RD, Fuld PA, Katzman R, Peck A. Pathological verification of ischemic score in differentiation of dementias. Ann Neurol 1980; 7: 486–8.

Scher AI, Xu Y, Korf ES, White LR, Scheltens P, Toga AW, et al. Hippocampal shape analysis in Alzheimer's disease: a population-based study. Neuroimage 2007; 36: 8–18.

Schonheit B, Zarski R, Ohm TG. Spatial and temporal relationships between plaques and tangles in Alzheimer-pathology. Neurobiol Aging 2004; 25: 697–711.

Strange BA, Fletcher PC, Henson RN, Friston KJ, Dolan RJ. Segregating the functions of human hippocampus. Proc Natl Acad Sci USA 1999; 96: 4034–9.

Tamamaki N, Nojyo Y. Disposition of the slab-like modules formed by axon branches originating from single CA1 pyramidal neurons in the rat hippocampus. J Comp Neurol 1990; 291: 509–19.

Thompson PM, Hayashi KM, de Zubicaray G, Janke AL, Rose SE, Semple J, et al. Dynamics of gray matter loss in Alzheimer's disease. J Neurosci 2003; 23: 994–1005.

Thompson PM, Hayashi KM, De Zubicaray GI, Janke AL, Rose SE, Semple J, et al. Mapping hippocampal and ventricular change in Alzheimer disease. Neuroimage 2004; 22: 1754–66.

Thompson PM, Schwartz C, Toga AW. High-resolution random mesh algorithms for creating a probabilistic 3D surface atlas of the human brain. Neuroimage 1996; 3: 19–34.

Trillo L, Gonzalo LM. Ageing of the human entorhinal cortex and subicular complex. Histol Histopathol 1992; 7: 17–22.

Van Hoesen GW, Hyman BT. Hippocampal formation: anatomy and the patterns of pathology in Alzheimer's disease. Prog Brain Res 1990; 83: 445–57.

Downloaded from https://academic.oup.com/brain/article/131/12/3266/296136 by guest on 20 April 2024

Wang L, Miller JP, Gado MH, McKeel DW, Rothermich M, Miller MI, et al. Abnormalities of hippocampal surface structure in very mild dementia of the Alzheimer type. Neuroimage 2006; 30: 52–60.

Wang L, Swank JS, Glick IE, Gado MH, Miller MI, Morris JC, et al. Changes in hippocampal volume and shape across time distinguish dementia of the Alzheimer type from healthy aging. Neuroimage 2003; 20: 667–82.

West MJ, Gundersen HJ. Unbiased stereological estimation of the number of neurons in the human hippocampus. J Comp Neurol 1990; 296: 1–22.

Downloaded from https://academic.oup.com/brain/article/131/12/3266/296136 by guest on 20 April 2024